



Thermal damage and mechanical properties of high temperature sandstone with cyclic heating–cooling treatment

Shaokun Ge¹ · Bobo Shi¹ · Shuai Zhang² · Xiaowei Zhai³ · Chunlei Wu¹

Received: 26 July 2021 / Accepted: 15 June 2022 / Published online: 24 June 2022
© Springer-Verlag GmbH Germany, part of Springer Nature 2022

Abstract

In the coal fire control project, the multiple water injections used to extinguish coal fires and the coal fires that reignite can cause many forms of ground collapse to occur, threatening project safety. Therefore, studying the thermal damage and the mechanical strength of sandstone, a main weight bearer in coal measure strata, exposed to heating–cooling cycles, is crucial. In this study, the sandstones were first heated to 800 °C and cooled using water. The sandstones were heated to a setting temperature (100 °C, 200 °C, 300 °C, 400 °C, 500 °C, 600 °C, 700 °C, and 800 °C) and cooled using water again. The ultrasonic p-wave velocity, density, and water absorption of the sandstones were tested. Uniaxial compression tests and shear tests were conducted on the sandstones. The thermal damage in sandstones was analysed using rock energy theory. The results show that, compared with the mechanical strength of the sandstone at room temperature, the mechanical strength of the sandstone exposed to 800 °C for the first time is decreased by less than 20%. When the sandstone is exposed to high temperature again, the critical threshold temperature is 400 °C. When the temperature exceeds 400 °C, the thermal damage aggravated again and the mechanical strength rapidly degraded.

Keywords Thermal damage · Mechanical property · Heating–cooling cycle · Energy evolution · Thermal expansion

Introduction

A considerable proportion of the energy in China is generated from coal and this will continue to remain the same (Li et al. 2020b). Spontaneous combustion of coal (coal fires) occurs frequently in shallow coal fields located in Xinjiang province, Ningxia, and Shaanxi provinces and other places in China (Deng et al. 2021; Shao et al. 2021) where coal resources are being burnt continuously (Deng et al. 2020; Zhou et al. 2015). The temperatures at coal fire centres exceed 800 °C (Deng et al. 2020; Shi et al. 2017),

transforming the surrounding rock into a high-temperature rock mass. In the coal fire control project, the grouting or watering used to extinguish fires (Zhou et al. 2015) rapidly cools the high-temperature rock. However, the rock could be heated up to a certain temperature owing to the coal reburning. The re-suppression of recrudescence is necessary to eliminate coal fires. Sandstone is an important load-bearing constituent of coal measure strata. Various types of ground collapses (Fig. 1) that occur in the process of repeated water injection are accompanied by sandstone breaking, which seriously threatens the safety of the coal fire control project. The collapses indicate that the thermal damage in sandstone re-exposed to high temperatures has increased and that the mechanical strength of the sandstone has weakened.

High-temperature sandstone is involved in various geological engineering applications, such as nuclear waste disposal (Mahanta et al. 2020), geothermal resource exploitation (Ranjith et al. 2012), coal mining (Pathiranagei and Gratchev 2021) and underground coal gasification (Xiao et al. 2021a). Thus, a study on the thermal damage and its effect on the mechanical strength of the rock will be important. The conclusions made by related previous studies could be divided into three categories. First, the

✉ Bobo Shi
shibobo@cumt.edu.cn

¹ School of Safety Engineering, China University of Mining and Technology, No.1 University Road, Xuzhou, Jiangsu 221116, People's Republic of China

² College of Energy Science and Engineering, Xi'an University of Science and Technology, Xi'an, Shaanxi 710054, People's Republic of China

³ College of Safety Science and Engineering, Xi'an University of Science and Technology, Xi'an, Shaanxi 710054, People's Republic of China



Fig. 1 Photographs of surface collapses that have occurred in the coal fire control project site after grouting/watering was used to extinguish coal fires in Shaanxi Province, China, showing the following: **a** single crack; **b** surface subsidence; and **c** crack zone

mechanical strength of sandstone degrades with increasing temperature and it almost loses its bearing capacity at 800 °C (Li et al. 2020a; Kong et al. 2016). Second, the strength of sandstone increases with temperature up to 400 °C and rapidly degrades at temperatures exceeding 400 °C. The mechanical strength of sandstone at 800 °C is less than that of raw sandstone by more than 40% (Mahanta et al. 2020; Sirdesai et al. 2017). In two categories of conclusions, 400 °C is considered a threshold temperature with respect to the thermal damage and mechanical strength of sandstone. As for the third conclusion, Fig. 2 shows a different characteristic that the mechanical compressive strength of the sandstone at temperatures below 800 °C increases slightly with temperature (Ranjith et al. 2012; Wei et al. 2019; Shi et al. 2020; Fan et al. 2022; Xiao et al. 2021a, b). Among that, the results of Wei et al. (2019), Shi et al. (2020), and Fan et al. (2022) showed that the strength of sandstone between 600 and 800 °C

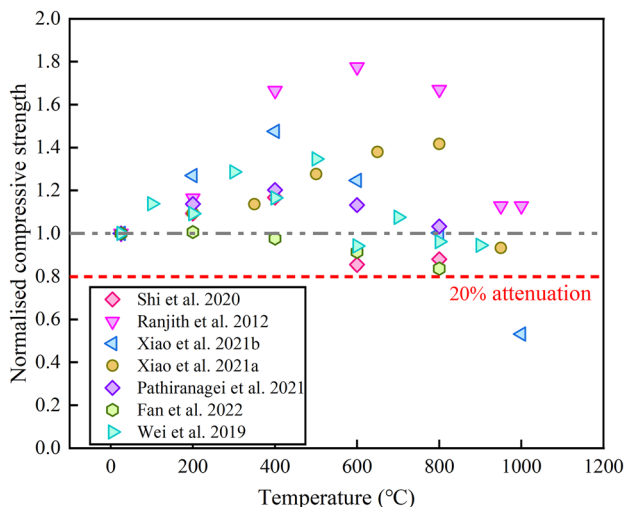


Fig. 2 Relationship between normalized compressive strength of sandstone and its temperature as reported in the literature

decays compared with the raw sandstone, but the attenuation does not exceed 20%. Differences in the structure of raw sandstone and various treatments to which they have been subjected to during the experiments may be contributing to these differentiated conclusions. Figure 2 depicts that at temperatures below 800 °C, the mechanical strength of the sandstone that has undergone one cycle of heating and cooling slightly degrades; therefore, it can sustain its load-bearing capacity. However, when re-ignition of coal fires occurs at control project sites, the cooled sandstone is heated again up to a certain temperature and can be cooled again through re-watering. Little attention has been paid to the thermal damage caused to the sandstone by exposing it to several heating–cooling cycles and how the mechanical strength of sandstone gets affected under those conditions. Therefore, it is necessary to study the failure mechanism of the sandstone subjected to heating at different temperatures after reaching a high temperature.

The critical temperature threshold of the sandstone experiencing the effects of changes in temperature for the first time was between 400 and 600 °C (Sun et al. 2020; Shen et al. 2021; Mahanta et al. 2020). In addition, Sun et al. (2020) reported that when sandstone is treated thermally, its thermal damage increases and its mechanical strength decreases. The influence of thermal cycles is not considerable at temperatures <400 °C. Pathiranagei and Gratchev (2021) observed similar behaviour in sandstone and emphasised that the decrease in rock strength cannot be neglected at temperatures exceeding 600 °C. Their study findings indicated that a threshold temperature should be considered in thermal cycling experiments. Combined with the phenomenon on coal fire control site, this paper speculates that there exists a critical temperature threshold for sandstone that has experienced 800 °C temperature once. The sandstone's mechanical strength begins to deteriorate when the temperature is increased beyond the critical temperature threshold. Thus, a study on the temperature threshold would enable a detailed understanding of the failure mechanism of thermally cycled sandstone.

In this context, the geology of the coal fire control project site with a complex high-temperature environment was considered the research background. The sandstone samples collected from the coal fire area were first heated to 800 °C and cooled using water. Second, the rock samples were heated to a set of temperatures (100 °C, 200 °C, 300 °C, 400 °C, 500 °C, 600 °C, 700 °C, and 800 °C) and cooled using water. Third, the ultrasonic p-wave velocity (v), density (ρ), and water absorption (w) of the sandstone samples were tested to determine the thermal damage caused to the samples. The uniaxial compression and shear tests were conducted to study the variation in the mechanical properties of the sandstone samples. Rock energy and energy dissipation theories were used to assess the thermal damage in the samples.

Materials and methods

Sandstone sample preparation

Sandstones were collected from the Sandaoba coal fire zone in Urumqi, Xinjiang Province, China. To facilitate the ease of transportation, the sandstones were processed on site and cube blanks with a size of 300 mm × 300 mm × 300 mm ($L \times W \times H$) were obtained. The samples were made from the blanks at the laboratory. They were of two sizes: 50 mm × 100 mm ($\varnothing \times h_1$), and 60 mm × 60 mm × 40 mm ($l \times w \times h_2$) in the laboratory. The samples with a size of 50 mm × 100 mm ($\varnothing \times h_1$) were used in the uniaxial compression test. The rest of the samples were prepared for the uniaxial shear test. The geological characteristics of the coal seam and sandstone samples are depicted in Fig. 3.

Laboratory equipment

Figure 4a–c depict the ultrasonic p-wave speed detector used to measure the ultrasonic p-wave velocities in the samples, KSL-1200X muffle furnace (with a maximum temperature of 1200 °C) used to heat the samples, and the electric blast drying oven used to dry the samples,

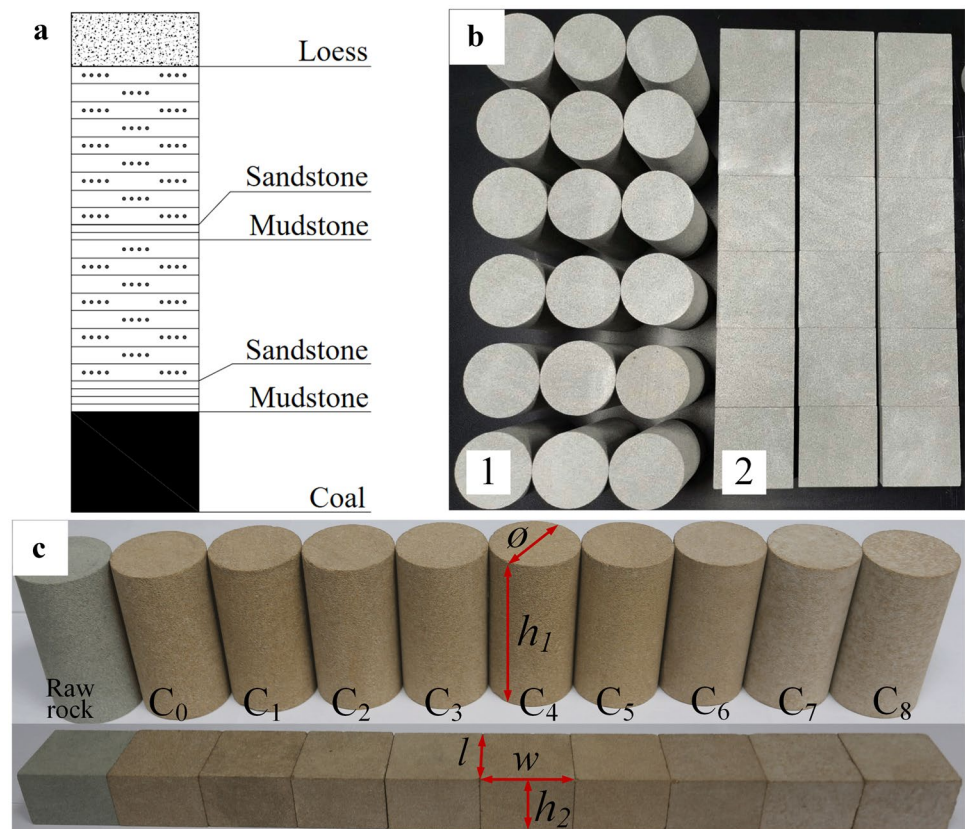
respectively. Figure 4d shows the electro-hydraulic servo universal testing machine used in the uniaxial compression and shear tests.

Experimental method and procedure

Cyclic heating–cooling of sandstone samples

Figure 5 depicts that the sandstone samples were treated under working conditions 0 (C_0) and n (C_n) with n falling between 1 and 8. During C_0 treatment, the samples were first slowly heated to 800 °C and maintained at that temperature for 2 h. Second, the samples were quickly removed from the high-temperature atmosphere furnace and placed in cooling water to enable them to cool to room temperature (25 °C). Last, the cooled samples were collected and dried. Under working condition 4 (C_4), the samples that had been exposed to working condition C_0 were slowly heated to 400 °C and kept at that temperature for 2 h. Then, the samples were quickly placed in water to cool them to room temperature (25 °C). To prevent hot rocks from influencing the water temperature, the flowing water was used to cool the samples. Sample processing is illustrated in Fig. 5.

Fig. 3 **a** Stratigraphic histogram of Sandaoba coal fire zone in Urumqi, Xinjiang Province, China; **b** sandstone samples before they underwent cyclic heating–cooling treatment; and **c** sandstone samples after they underwent cyclic heating–cooling treatment. Notes: Group 1. Samples used in the uniaxial compression test and Group 2. Samples used in the uniaxial shear test



Experimental procedure

The ultrasonic p-wave velocities in the sandstone samples before the samples underwent cyclic heating–cooling were measured. The samples that had differing wave velocities were removed and the remaining sandstone samples were numbered. The numbered samples were weighed and measured to obtain the density of the raw sandstone.

The samples were pre-treated by subjecting them to cyclic heating–cooling. Ersoy et al. (2019) reported that the heating rate was set at 3 °C/min to reduce thermal damage in the samples due to rapid heating. The C₀ samples were placed in the electric blast drying oven and dried for 24 h. The weight, volume, and p-wave velocity of the dried samples were measured immediately after being dried. The C_n samples were removed from the water and kept in a ventilated area for 30 min to remove their surface water. The mass of each sample was obtained to determine the amount of water absorption. Then, the samples were re-dried to analyse the variation in their wave velocities. Finally, the uniaxial compression and shear tests were performed on the samples.

In the uniaxial compression test, the load applied to the rock samples was controlled using axial displacement, which changed at the rate of 0.002 mm/s. In the shear test, the load was changed using axial compression at a loading rate of 3000 N/s. The shear angle was set at 45°. The test was terminated when the sample surfaces collapsed.

Sandstone parameter definitions

For quantitative analysis of the variations in physical parameters of the sandstone, the rate of change of ultrasonic p-wave velocity was defined as k_v (Eq. (1)). The change in the water absorption rate was defined as k_w (Eq. (2)) given as follows:

$$k_v = \frac{v_n - v_0}{v_0} \times 100\% \quad (1)$$

$$k_w = \frac{w_n - w_0}{w_0} \times 100\% \quad (2)$$

$$w_n = \frac{m_{n0} - m_n}{m_n} \times 100\% \quad (3)$$

where v_0 and v_n are the ultrasonic p-wave velocities of C₀ and C_n sandstone samples, respectively; w_0 and w_n are the water absorption rates of the C₀ and C_n sandstone samples, respectively and m_{n0} and m_n are the undried and dried mass of C_n sandstone, respectively.

Results

Variation in sandstone physical properties

Appearance of sandstone

As shown in Fig. 3c, raw sandstone is grey, whereas sandstone that has undergone cyclic heating and cooling is tawny. No cracks can be seen on the surface of pre-treated sandstone. The surface colour of the C₁–C₄ samples (100–400 °C) is not distinctly different from that of C₀ samples. However, the colours of C₅–C₈ samples (500 °C–800 °C) change considerably. The colour becomes pale when the temperature exceeds 400 °C. The change in the sample colour can be attributed to the chemical reactions of metallic elements, such as iron (Ersoy et al. 2019; Shen et al. 2021; Shi et al. 2021), contained in the samples. The chemical reactions that can be expressed using Eqs. (4) and (5) occur in iron during thermal cycling, causing the samples to turn red because of the presence of red Fe₂O₃.



Changes in the physical parameters of sandstone

Table 1 lists the physical parameters of the samples measured in the uniaxial compression test. The density and p-wave velocity of raw sandstone exceed those of C₀ sandstone. The water absorption of raw sandstone is less than that of C₀ sandstone. These changes are caused by the thermal damage that occurs when the samples are subjected to high temperature and water cooling. Figure 6 presents the relationship between density, k_v , k_w and the temperature of

Table 1 Physical parameters of 50 mm × 100 mm ($\varnothing \times h_l$) sandstone samples

Name	Condition	p-wave velocity (km/s)	m_{n0} (g)	m_n (g)	Volume (cm ³)
NY1,2,3	25 °C	3.03	451.25	433.73	186.27
0Y1,2,3	C ₀	1.61	455.78	427.35	190.62
1Y1,2,3	C ₁	1.58	455.61	427.02	190.15
2Y1,2,3	C ₂	1.60	456.53	427.97	190.67
3Y1,2,3	C ₃	1.54	456.21	427.19	190.67
4Y1,2,3	C ₄	1.56	457.05	427.84	190.42
5Y1,2,3	C ₅	1.41	458.33	427.63	190.89
6Y1,2,3	C ₆	1.35	459.69	427.87	191.14
7Y1,2,3	C ₇	1.28	459.26	427.32	191.32
8Y1,2,3	C ₈	1.21	460.07	427.21	192.41

Fig. 4 **a** Ultrasonic p-wave speed detector. **b** KSL-1200X muffle furnace. **c** Electric blast drying oven. **d** Electro-hydraulic servo universal testing machine



the samples. The temperature affects the sandstone in two stages. The first stage is between 100 and 400 °C, and the second stage is between 500 and 800 °C. In the first stage, the temperature increases but ρ fluctuates around 2.242 g/cm³, indicating that ρ is insensitive to temperature. In the second stage, the temperature is above 400 °C and ρ decreases sharply as the temperature increases, indicating a negative linear relationship with temperature. ρ is reduced to 2.232 g/cm³ at 800 °C. The p-wave velocity and water absorption of sandstone are related to ρ . In the second stage, k_v changes from -2.49 to -24.85%. k_w increases from 1.42 to 15.62%, indicating a positive linear correlation with temperature. This synergistic change indicates that new cracks occur and expand inside sandstone in the second stage (Yavuz et al. 2010).

Uniaxial compression test

Stress–strain curve characteristics of thermally cycled sandstone

Figure 7 depicts the typical stress–strain curves of thermally cycled sandstone. The initial compression stage, non-linear elastic stage, linear elastic stage, yield stage and post-peak failure stage of sandstone are represented in the stress–strain curves by the segments OA, AB, BC, CD, and DE, respectively. In the first stage of C₁, C₂, C₃, and

C₄ sandstone samples, the strain values (ϵ_{OA}) are approximately equal and are less than 0.004, which indicates that during the 100–400 °C heating–cooling cycle, no damage occurs in sandstone samples. Almost no new micro-cracks occur in sandstones (Ersoy et al. 2021; Sirdesai et al. 2017). In the second stage of C₅, C₆, C₇, and C₈ sandstone samples, ϵ_{OA} becomes considerably long and exhibits a growing trend as temperature increases, which indicates the presence of new micro-cracks. The thermal damage increases as the temperature increases beyond 400 °C (Sirdesai et al. 2017).

In the first stage, ϵ_{AB} , ϵ_{BC} , and ϵ_{CD} are almost equal. However, in the second stage, the three parameters change considerably as the temperature increases: ϵ_{AB} and ϵ_{CD} become longer and ϵ_{BC} becomes shorter. The stress corresponding to point C decreases gradually. The phenomenon implies that the deformation of sandstone increases under the same stress load. The failure mode of sandstone changes from brittle to ductile (Kong et al. 2016) and the plastic deformation of sandstone increases; however, its load-bearing capacity decreases (Li et al. 2020a).

Mechanical characteristics of the sandstone subjected to thermal cycling

Table 2 lists the mechanical parameters of sandstone samples recorded during the uniaxial compression test. Figures 8 and 9 present the variation with temperature in peak stress, elastic modulus, peak strain and the Poisson’s ratio of sandstone samples subjected to different thermal cycles. The changes in the mechanical strength are not noticeable in the first stage. The peak stress, elastic modulus, peak strain and the Poisson’s ratio fluctuate slightly from 50.00 to 50.95 MPa, 6.94 to 7.07 GPa, 0.0144 to 0.0147, and 0.20 to 0.22, respectively. In the second stage, the mechanical strength deteriorates rapidly as temperature increases. Compared with sandstones under C₀, the values of peak stress and elastic modulus decrease by 5.0–19.7% and 11.0–21.1%, respectively. However, the percentage increase in peak strain and the Poisson’s ratio is between 14.5 and 33.1% and between 30.0 and 70.0%, respectively. The compressive strength behaviour confirms that plastic deformation of the sandstones increases and ductile failure occurs during the second stage.

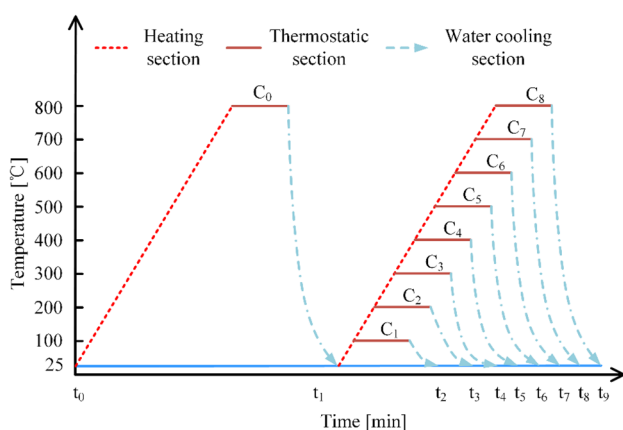


Fig. 5 Cyclic heating–cooling treatments of different groups of sandstone samples

Table 2 Mechanical parameters of 50 mm × 100 mm ($\varnothing \times h_f$) sandstone samples

Name	Condition	Peak stress (MPa)	Peak strain (10^{-2})	Elastic modulus (GPa)	Poisson's ratio	Shear stress (MPa)
NY1,2,3	25 °C	63.42	1.06	9.41	0.38	34.52
0Y1,2,3	C ₀	51.03	1.45	7.06	0.20	31.93
1Y1,2,3	C ₁	50.90	1.44	7.03	0.20	31.65
2Y1,2,3	C ₂	50.13	1.46	7.01	0.22	31.86
3Y1,2,3	C ₃	50.00	1.47	7.07	0.20	31.39
4Y1,2,3	C ₄	50.95	1.44	6.94	0.22	31.47
5Y1,2,3	C ₅	48.48	1.66	6.28	0.26	30.51
6Y1,2,3	C ₆	47.19	1.74	6.10	0.28	29.81
7Y1,2,3	C ₇	45.13	1.85	5.95	0.32	29.55
8Y1,2,3	C ₈	40.97	1.93	5.57	0.34	27.17

Shear test

The shear test results of the sandstone samples are depicted in Fig. 10. In the first stage, the shear strength is between 31.39 and 31.86 MPa and it has been hardly affected by temperature. In the second stage, the shear strength decreases rapidly with increasing temperature reaching 27.12 MPa at 800 °C. The shear strength of C₅–C₈ samples is reduced by 4.4 ~ 14.9% compared with that of the C₀ sandstone. Compared with the uniaxial compression strength at any particular temperature, the shear strength has a smaller attenuation at the same temperature. This phenomenon could be attributed to the different loading methods used in the two sets or to sample size differences. The variation patterns of shear strength and uniaxial compressive strength are similar. The reasons for the decrease in the shear and compressive strengths would be discussed in detail in the “Discussion” section.

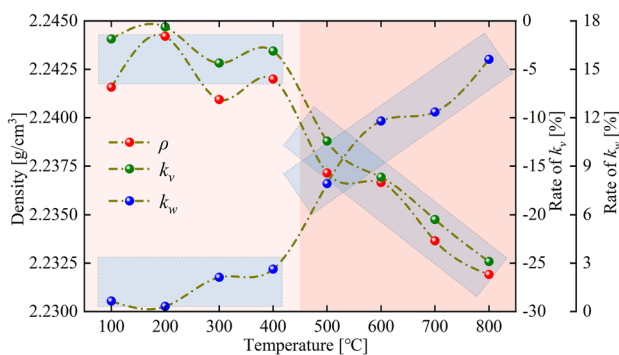


Fig. 6 Relationship between the physical parameters (ρ , k_v , k_h) of thermally cycled sandstone with temperature

Effects of thermal cycling on the energy evolution law of sandstone

The damage of loaded rock is accompanied by energy evolution that reflects the crack expansion and damage evolution inside the rock (Han et al. 2020; Luo et al. 2020; Xie et al. 2009; Zhang et al. 2020a). It specifically includes the following two aspects: (1) the original cracks, including the cracks caused by thermal damage, are reflected by the strain energy dissipated during the initial compression and non-linear elastic stages (Luo et al. 2020; Zhang et al. 2020a) and (2) the increase in the energy at the yield stage, implying the formation of new cracks (Qin et al. 2020; Zhang et al. 2020b). Luo et al. (2020) concluded that the work required for the propagation of rock cracks during compression could be quantified using the dissipated strain energy. A high proportion of the strain energy dissipated in the stages preceding the yield stage indicates that the rock has numerous inherent cracks. Cracks formed in high-temperature rocks are of two forms: structural cracks and thermally induced cracks. If the structural cracks can be assumed almost similar, the exacerbated thermal damage of high-temperature sandstone can be represented by an increase in the dissipated strain energy before reaching the yield stage.

Rock energy theory

The discussion that follows is based on the uniaxial compression test results. If energy dissipation, such as that caused by the friction between sandstone sample and testing machine, is neglected, the samples can be assumed to completely absorb the work of the testing machine. In this study, the work was recorded as the total strain energy (U ; Han et al. 2020; Xie et al. 2009). Part of U , defined as the elastic strain energy (U^e), will be stored in the elastic structure of sandstone (Han et al. 2020). The energy remaining is the dissipated strain energy (U^d).

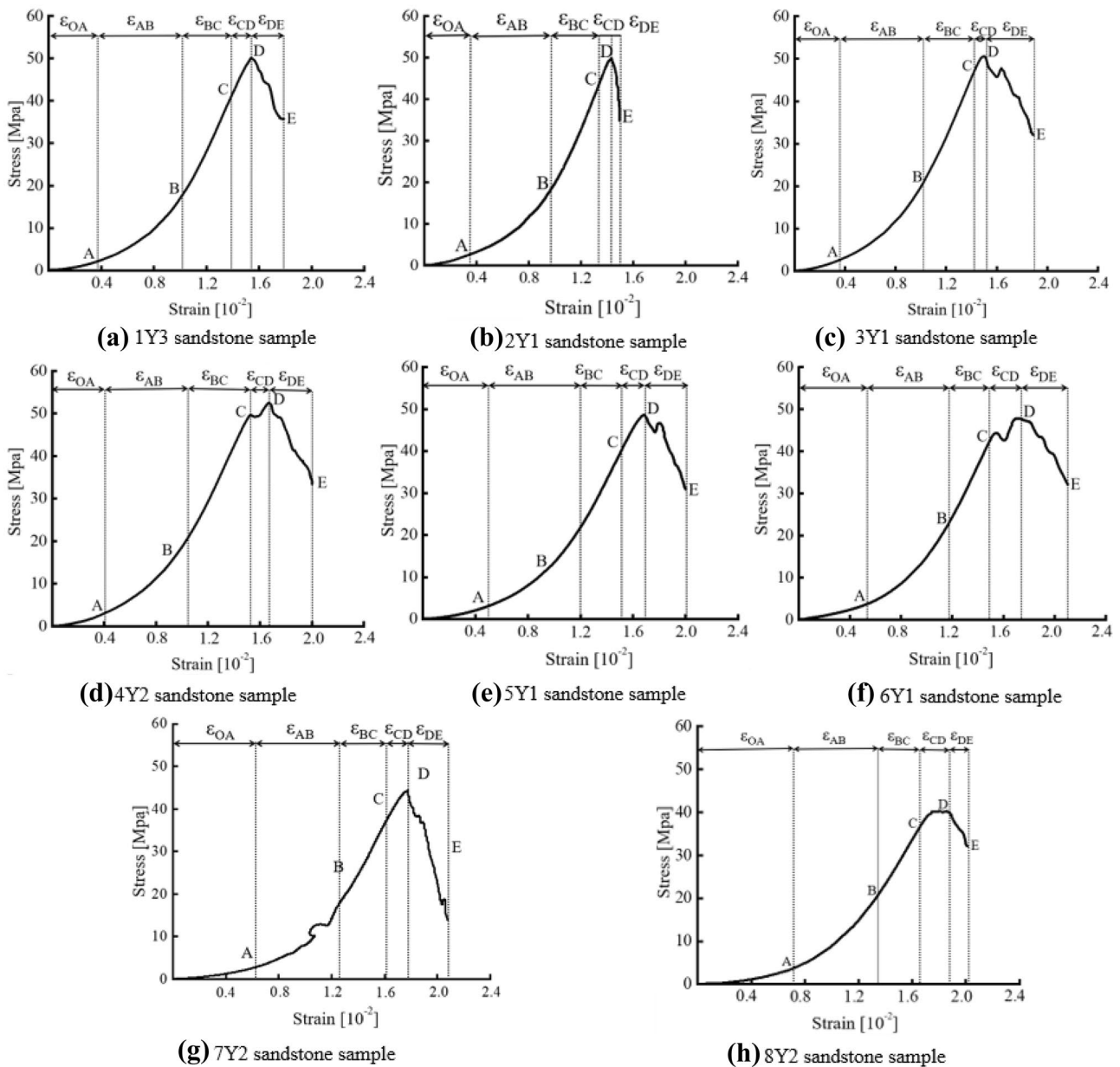


Fig. 7 Stress–strain curves of sandstone exposed to different thermal cycles

Based on the relationship between work and energy, U can be calculated by integrating the stress–strain curve of the sandstone sample (Eq. (6)).

$$U = \int \sigma_1 d\epsilon_1 = \sum_{i=0}^n \frac{1}{2} (\epsilon_{1i+1} - \epsilon_{1i}) (\sigma_{1i} + \sigma_{1i+1}) \quad (6)$$

The energy relationship at time I during compression can be expressed using Eq. (7) as follows:

$$U_i = U_i^e + U_i^d \quad (7)$$

Equations (8) and (9) can be obtained using Hooke’s law as follows:

$$U_i^e = \frac{1}{2} \sigma_{1i} \epsilon_{1i}^e \quad (8)$$

$$\sigma_{1i} = E_{1i} \cdot \epsilon_{1i}^e \quad (9)$$

Thus, U^e can be calculated using Eq. (10) as follows:

$$U_i^e = \frac{1}{2} \sigma_{1i} \epsilon_{1i}^e \approx \frac{\sigma_{1i}^2}{2E_0} \quad (10)$$

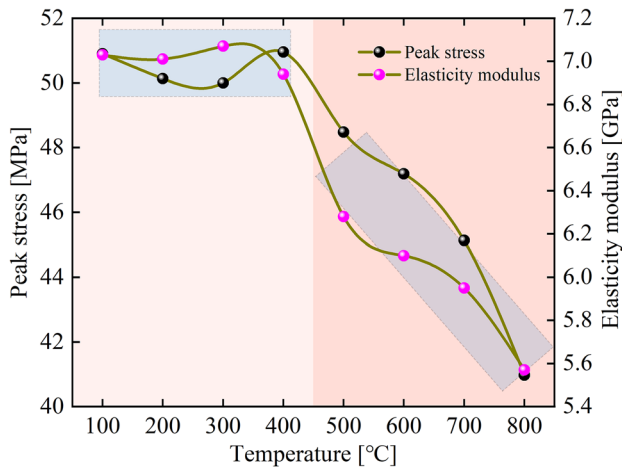


Fig. 8 Relationship between temperature and the peak stress and elasticity modulus of thermally cycled sandstone

where σ_i and ϵ_i represent the stress and strain in the samples, respectively, during the uniaxial compression test; σ_{li} and ϵ_{li} represent the stress and strain at time i of the stress–strain curve, respectively; n represents the total number of counting points; $\epsilon \epsilon l i$ represents the elastic strain at time i ; E_{li} represents the elasticity modulus of sandstone at time i and E_0 represents the elastic modulus of sandstone in the BC segment of the stress–strain curve.

Energy consumption characteristics of sandstone under the influence of temperature

The C_5 and C_8 sandstone samples were selected to illustrate the energy consumption law. In Fig. 11, the curves of U , U^e and U^d show different characteristics in different

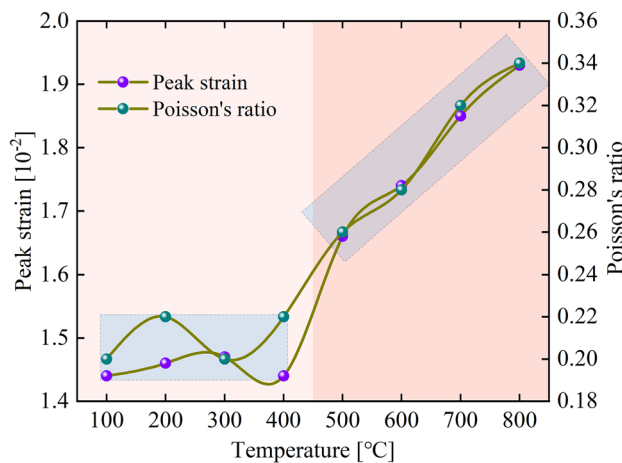


Fig. 9 Relationship between temperature and the peak strain and the Poisson's ratio of thermally cycled sandstone

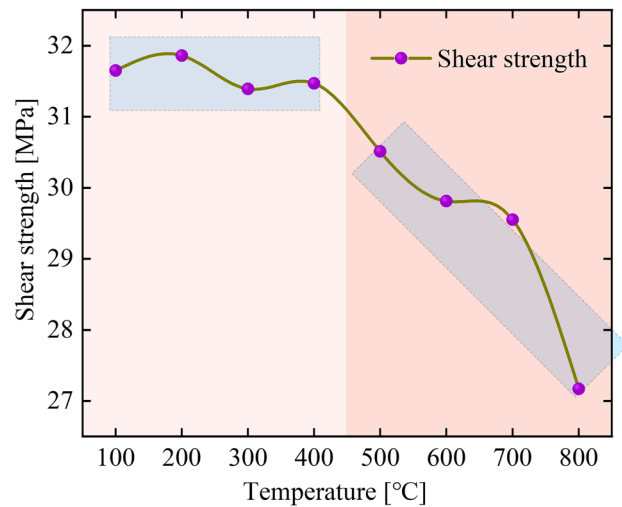


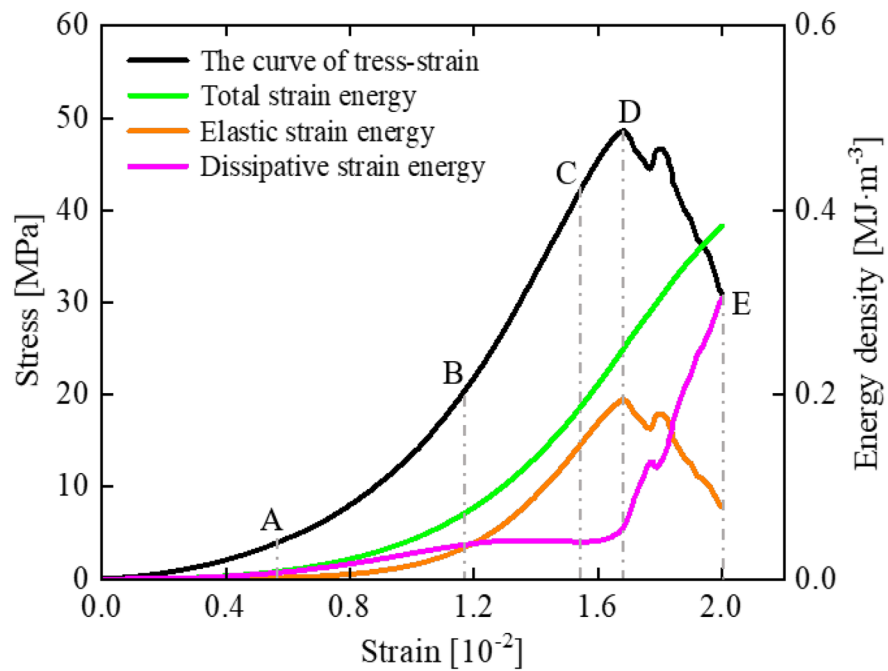
Fig. 10 Relationship between temperature and the shear strength of sandstones with thermal cycle treatment

segments. In the OA segment, U , U^e and U^d increase slowly. In the AB segment, U^d exceeds U^e within the unit strain (the original cracks in the samples are compacted again and consume most of U). The original cracks intersect at point B. In the BC segment, U^e shows a linear and rapid growth with strain. However, U^d hardly increases, indicating that only a few new cracks have developed. This result is consistent with the conclusions reported by Qin et al. (2020). In the CD segment, the growth rate of U^e decreases and U^d increases slowly. Thus, new micro-cracks have appeared because of external forces (Zhang et al. 2020a). When raw cracks penetrate the new cracks (point D), the stress attains its peak value and the sandstone is damaged. In the DE segment, U^e decreases rapidly while U^d increases. U^e is released as the sandstone fails. Particularly, U^e appears as a ‘platform’ in the CD segment of the stress–strain curve of the sample heated to 800 °C, which indicates that ductile failure has occurred in the sample.

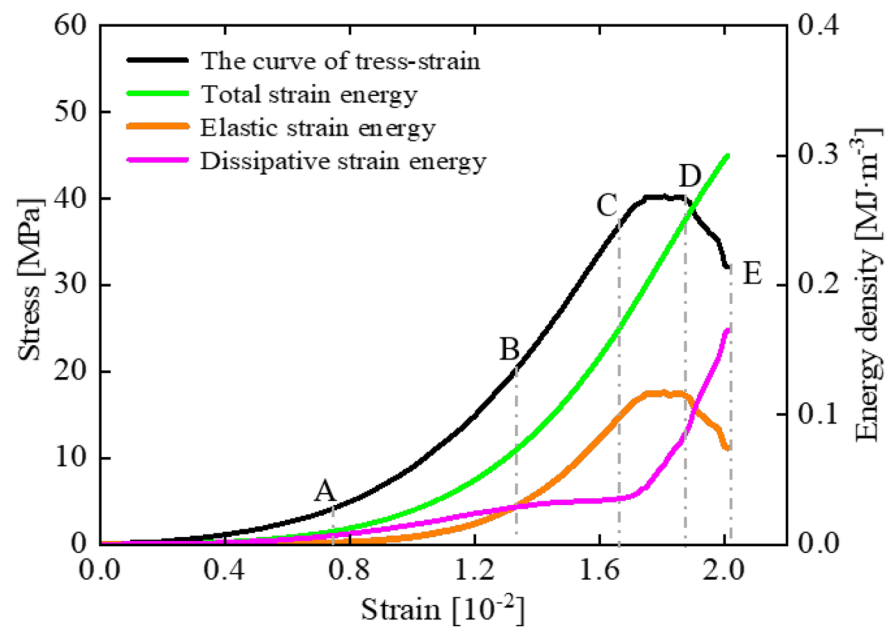
Relationship between U^d and thermal damage in the high-temperature sandstone

The relationship between U^e and U^d and the temperature of sandstone samples before reaching the yield stage is shown in Fig. 12. They hardly change during the first stage. During the second stage, as the temperature increases, the proportion of U^d increases. The U^d proportion in C_5 sandstone is 8.40% greater than that of C_4 sandstone. The increasing proportion of U^d indicates an increase in the micro-cracks within the sandstone. The sandstones with evident differences in p-wave velocity were removed as

Fig. 11 Energy evolution characteristics with the strain of sandstone samples



(a) Energy evolution characteristics with strain of 5Y1 sandstone sample



(b) Energy evolution characteristics with strain of 8Y2 sandstone sample

mentioned in the “[Experimental procedure](#)” section. The number of structural cracks in the remaining sandstone can be approximately equal. Thermal cycling causes an increase in the internal cracks in the sandstone, resulting in increasing the U^d proportion before reaching the yield stage. Therefore, the increasing U^d proportion demonstrates that the thermal damage has intensified starting from 400 °C.

Discussion

In this study, the uniaxial compressive and shear strengths of raw sandstone were chosen as 63.42 and 34.52 MPa, respectively. The compressive and shear strength of sandstone exposed to 800 °C for the first time (C_0) were 51.03 and 31.39 MPa, respectively. They were attenuated by 19.53% and 9.07%, respectively, indicating that load-bearing

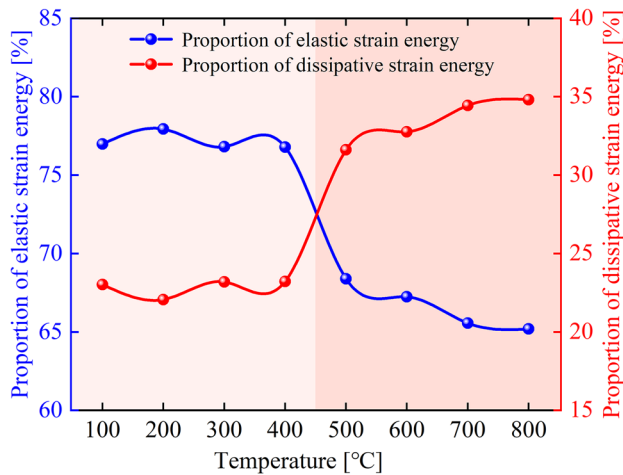


Fig. 12 Relationship between U^e and U^d and temperature of sandstone samples before reaching the yield stage

capacity of sandstone has not considerably decreased. Thus, no surface cracks would appear at the coal fire-extinguishing site before repeated water injection is commenced. When sandstone is exposed to high temperatures again, the thermal damage in the sandstone and mechanical strength of the sandstone begins to change as the temperature rises again above 400 °C.

Thermal damage in sandstone subjected to cyclic heating-cooling treatment

Sandstone comprises several minerals, such as quartz, kaolinite, plagioclase, and calcite, which have different thermal expansion coefficients (McCabe et al. 2010; Crosby et al. 2018; Ersoy et al. 2019; Sun et al. 2020). Temperature affects the thermal expansion of minerals (Mahanta et al. 2016; Kumari et al. 2017; Ersoy et al. 2021). At temperatures below 400 °C, the negligible difference in thermal expansion does not lead to new cracks and does not weaken sandstone mechanical strength (Pathiranagei and Gratchev 2021; Sun et al. 2020). When the temperature exceeds 400 °C, the differential thermal expansion causes thermal stress within the rock, promoting the formation of new cracks (Kumari et al. 2017; Ersoy et al. 2019; Shen et al. 2020). When the high-temperature sandstone is cooled by water, a large temperature gradient occurs inside the rock, which promotes un-coordinated thermal expansion and aggravates rock strength attenuation (Tao et al. 2018; Fan et al. 2022). In addition, high temperatures cause mineral-to-thermal phase transformation in sandstone (Kumari et al. 2017; Pathiranagei and Gratchev 2021). For example, α -quartz transforms into β -quartz at 573 °C (Chakrabati et al. 1996; Pathiranagei and Gratchev 2021), which further damages the rock micro-structure. When sandstone is

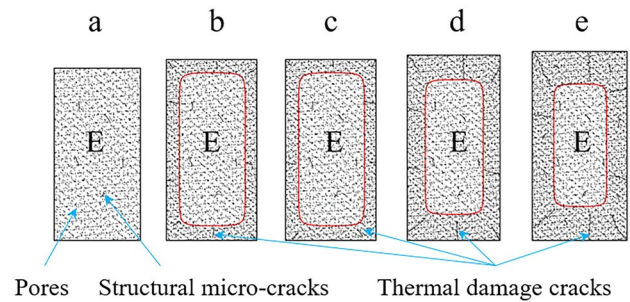


Fig. 13 Formation of thermal damage in sandstone. **a** Raw sandstone at room temperature. **b** Sandstone exposed to 800 °C for the first time. **c** Sandstone exposed to 100–400 °C for the second time. **d** Sandstone exposed to 500 °C for the second time. **e** Sandstone exposed to 800 °C for the second time

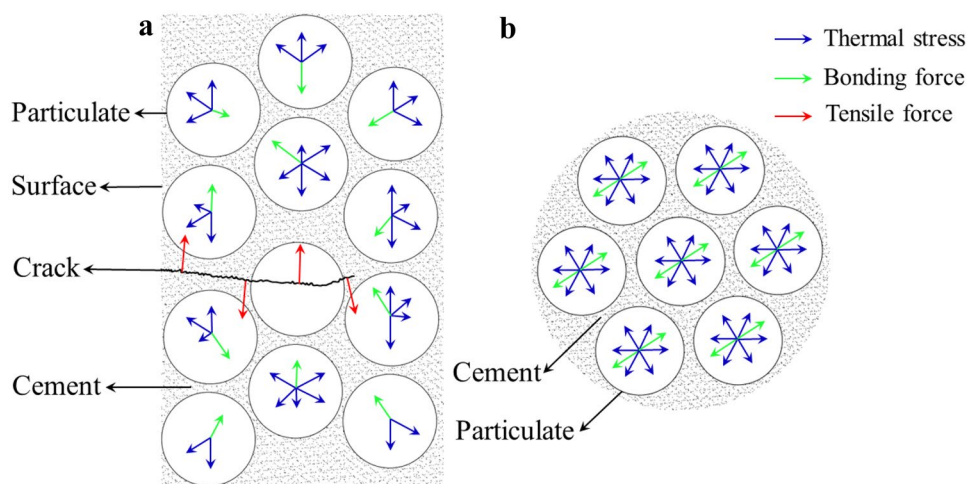
cooled, β -quartz reversely transforms into α -quartz (Shen et al. 2020). Water cooling causes a reverse thermal phase transition of the minerals, which again stimulates crack generation and propagation. The degree of inter-connection associated with internal cracks affects the physical properties and mechanical strength of sandstone.

During the heating of C_0 sandstone to 800 °C, the rock underwent uncoordinated thermal expansion and thermal phase transformation of its minerals successively. When sandstone was cooled using water, the cold shock was conducive to the continuous development of uncoordinated thermal expansion and reverse thermal phase transition. The thermal expansion and thermal phase change reduced the mechanical strength of C_0 sandstone by less than 20%. When the C_1 – C_8 sandstones were subjected to thermal cycles again, the thermal damage that occurred in the rock and the changes in its mechanical parameters were different. In C_1 – C_4 sandstone (the first stage), the thermal expansion was negligible and water cooling had no positive effect on the cracks. In C_5 – C_8 sandstone (the second stage), uncoordinated thermal expansion and reversible thermal phase transitions occurred because of the effects of temperature and water cooling, which increased the thermal damage and deteriorated its mechanical strength. Therefore, thermally cycled sandstone exposed to different temperatures after being heated to 800 °C has a critical threshold temperature of 400 °C.

Damage process of sandstone subjected to cyclic heating-cooling treatment

The main body (E), defined as the elastic core (Wang et al. 2014), of the rock with few cracks fully bears the applied load (Elkadi and Van Mier 2006). In this study, the entire raw sandstone was considered E. As illustrated in Fig. 13, the sandstone volume increases when sandstone is subjected to 800 °C for the first time. Un-coordinated thermal expansion of mineral particles occurs extending from the red line

Fig. 14 **a** Uncoordinated thermal expansion of mineral crystals on the rock surface. **b** Coordinated thermal expansion of mineral crystals in the E of rocks



to the sandstone surface, causing micro-crack creation (Shen et al. 2020). At the high temperature of 800 °C, uncoordinated thermal expansion occurs. Water cooling promotes the further development of thermal expansion. By contrast, the mineral particles of E within the red circle undergo coordinated expansion. The expansion and contraction volumes of each particle are equal, and no micro-cracks appear. In the first stage, the E of sandstone is not destroyed at low temperatures (100–400 °C) and when placed in cold water. When the temperature exceeds 400 °C in the second stage, the width and length of the micro-cracks outside the red circle increase because of the high temperature and water cooling. The expanded micro-cracks provide space for the un-coordinated expansion of the mineral particulates in E. As thermal damage increases, E shrinks and the mechanical strength decreases. This step-by-step process reveals that the damage caused by temperature and water cooling occurs only gradually starting from the surface and moving inwards. Peng et al. (2019) illustrated this process.

The causes of un-coordinated and coordinated thermal expansion of the mineral particles in sandstone are illustrated in Fig. 14. The particles undergo thermal expansion and are squeezed by thermal stress caused by the thermal expansion of other minerals and are simultaneously subjected to bonding forces of the cement (Shen et al. 2020). The thermal stress and bonding force of the surface particles of sandstone are not equal. The unbalanced force is converted into a tensile force, which destroys the particles and cement (Mahanta et al. 2016). Inter-granular and trans-granular micro-cracks will appear in the sandstone (Wang et al. 2017). Each mineral particle in the E is tightly wrapped around other particles. The thermal stress and bonding force of each mineral particle are equal. The particles expand and contract to the same extent without cracking. The thermal stress concentration is generated at the crack tips of sandstone subjected to high temperatures (>400 °C), promoting

crack expansion. The particles on either side of the crack undergo un-coordinated thermal expansion, worsening the thermal damage. Thus, as the temperature increases, the thermal damage in E of sandstone subjected to water cooling increases and its mechanical strength deteriorates.

Future research work

The thermal damage and mechanical properties of sandstone exposed to cyclic heating–cooling were investigated. The coordinated thermal expansion and un-coordinated thermal expansion were used to explain the damage process. Mathematical methods that can be used to analyse the thermal damage in sandstone are not available. Thus, a thermal damage assessment model should be developed. Our future research will attempt to express the relationship between temperature and thermal damage using a mathematical equation. It will help us understand quantitatively the effects of different cyclic heating–cooling conditions on high-temperature sandstone.

Conclusion

In this study, sandstone samples were heated to 800 °C and cooled using water. Then, they were heated to a set of temperatures (100 °C, 200 °C, 300 °C, 400 °C, 500 °C, 600 °C, 700 °C, and 800 °C) and cooled using water. Using uniaxial compression as well as shear test results and rock energy analysis, the thermal damage and mechanical properties of sandstone subjected to cyclic heating–cooling were determined. Moreover, the coordinated and uncoordinated thermal expansions of sandstone were used to identify the dynamic relationship between thermal expansion and crack development. The conclusions of this study are given as follows.

1. The effect of temperature on sandstone in a cyclic heating–cooling environment and exposed to a high temperature could be divided into two stages, demarcated at 400 °C. In the first stage (100–400 °C) of the second thermal cycle of sandstone already subjected to 800 °C once, the parameters, such as the surface colour, density, water absorption and ultrasonic p-wave velocity, showed almost no change. In the second stage (500–800 °C), the surface colour gradually became pale as the temperature increased. ρ and k_v had a negative linear correlation with temperature. ρ reduced to 2.232 g/cm³ and the ultrasonic p-wave velocity reduced by 24.85% at 800 °C. k_w had a positive linear correlation with temperature, increasing to 15.62% at 800 °C.
2. During the first stage, the reduction of compressive and shear strengths was not obvious. During the second stage, the peak stress and elastic modulus of sandstone decreased by 5.0–19.7% and by 11.0–21.1%, respectively. The attenuation of shear strength was between 4.4 and 14.9%. The peak strain and the Poisson's ratio increased by 14.5–33.1% and by 30.0–70.0%, respectively. Therefore, the critical threshold temperature of sandstone heated to different temperatures after being first heated to 800 °C was 400 °C.
3. During the first stage, the proportion of U^e and U^d in sandstone (before reaching the yield stage) hardly changed. During the second stage, the U^d proportion of C₅ sandstone exceeded that of C₄ sandstone treated by 8.40%. The U^d proportion increased as the temperature increased. The percentage of dissipated strain energy was consistent with the thermal damage in sandstone. The thermal damage aggravated after the temperature increased beyond 400 °C.

Author contribution Conceptualization, B.S.; writing—original draft preparation, B.S., S.G., S.Z.; validation, S.G., S.Z.; experimental and graphics: C.W., S.G., X.Z.; writing—review and editing, B.S., S.G., X.Z.; All authors have read and agreed to the published version of the manuscript.

Funding The work was supported by the National Natural Science Foundation of China (Grant No. 52074277) and the Natural Science Foundation of Jiangsu Province (Grant No. BK20211585).

Declarations

Conflicts of interest The authors declare no competing interests.

References

- Chakrabati B, Yates T, Lewry A (1996) Effect of fire damage on natural stonework in buildings. *Constr Build Mater* 10:539–544. [https://doi.org/10.1016/0950-0618\(95\)00076-3](https://doi.org/10.1016/0950-0618(95)00076-3)
- Crosby ZK, Gullett PM, Akers SA et al (2018) Characterization of the mechanical behavior of Salem limestone containing thermally-induced microcracks. *Int J Rock Mech Min Sci* 101:54–62. <https://doi.org/10.1016/j.ijrmms.2017.11.002>
- Deng JC, Ge SK, Qi HN et al (2021) Underground coalfire emission of spontaneous combustion, Sandaoba coalfield in Xinjiang, China: investigation and analysis. *Sci Total Environ* 777:146080. <https://doi.org/10.1016/j.scitotenv.2021.146080>
- Deng JC, Zhou FB, Shi BB et al (2020) Waste heat recovery, utilization and evaluation of coalfield fire applying heat pipe combined thermoelectric generator in Xinjiang, China. *Energy* 207:118303. <https://doi.org/10.1016/j.energy.2020.118303>
- Elkadi AS, Van Mier JGM (2006) Experimental investigation of size effect in concrete fracture under multiaxial compression. *Int J Fract* 144:55. <https://doi.org/10.1007/s10704-006-6728-7>
- Ersoy H, Atalar C, Sünnetci MO et al (2021) Assessment of damage on geo-mechanical and micro-structural properties of weak calcareous rocks exposed to fires using thermal treatment coefficient. *Eng Geol* 284:106046. <https://doi.org/10.1016/j.enggeo.2021.106046>
- Ersoy H, Kolaylı H, Karahan M et al (2019) Effect of thermal damage on mineralogical and strength properties of basic volcanic rocks exposed to high temperatures. *Bull Eng Geol Environ* 78:1515–1525. <https://doi.org/10.1007/s10064-017-1208-z>
- Fan LF, Li H, Xi Y (2022) Evaluation of the effects of three different cooling methods on the dynamic mechanical properties of thermal-treated sandstone. *Bull Eng Geol Environ* 81:154. <https://doi.org/10.1007/s10064-022-02630-1>
- Han DY, Li KH, Meng JJ (2020) Evolution of nonlinear elasticity and crack damage of rock joint under cyclic tension. *Int J Rock Mech Min Sci* 128:104286. <https://doi.org/10.1016/j.ijrmms.2020.104286>
- Kong B, Wang EY, Li ZH et al (2016) Electromagnetic radiation characteristics and mechanical properties of deformed and fractured sandstone after high temperature treatment. *Eng Geol* 209:82–92. <https://doi.org/10.1016/j.enggeo.2016.05.009>
- Kumari WGP, Ranjith PG, Perera MSA et al (2017) Temperature-dependent mechanical behaviour of Australian Strathbogie granite with different cooling treatments. *Eng Geol* 229:3144. <https://doi.org/10.1016/j.enggeo.2017.09.012>
- Li M, Wang DM, Shao ZL (2020a) Experimental study on changes of pore structure and mechanical properties of sandstone after high-temperature treatment using nuclear magnetic resonance. *Eng Geol* 275:105739. <https://doi.org/10.1016/j.enggeo.2020.105739>
- Li M, Wang HT, Wang DM et al (2020b) Experimental study on characteristics of surface potential and current induced by stress on coal mine sandstone roof. *Eng Geol* 266:105468. <https://doi.org/10.1016/j.enggeo.2019.105468>
- Luo Y, Wang G, Li XP et al (2020) Analysis of energy dissipation and crack evolution law of sandstone under impact load. *Int J Rock Mech Min Sci* 132:104359. <https://doi.org/10.1016/j.ijrmms.2020.104359>
- Mahanta B, Singh TN, Ranjith PG (2016) Influence of thermal treatment on mode I fracture toughness of certain Indian rocks. *Eng Geol* 210:103–114. <https://doi.org/10.1016/j.enggeo.2016.06.008>
- Mahanta B, Ranjith PG, Vishal V et al (2020) Temperature-induced deformational responses and microstructural alteration of sandstone. *J Petro Sci Eng* 192:107239. <https://doi.org/10.1016/j.petro.2020.107239>
- McCabe S, Smith BJ, Warke PA (2010) Exploitation of inherited weakness in fire-damaged building sandstone: the ‘fatiguing’ of ‘shocked’ stone. *Eng Geol* 115:217–225. <https://doi.org/10.1016/j.enggeo.2009.06.003>
- Pathiranagei SV, Gratchev I (2021) Engineering properties of sandstone heated to a range of high temperatures. *Bull Eng Geol Environ* 80:2415–2432. <https://doi.org/10.1007/s10064-020-02065-6>
- Peng J, Rong G, Tang ZC et al (2019) Microscopic characterization of microcrack development in marble after cyclic treatment with

- high temperature. *Bull Eng Geol Environ* 78:5965–5976. <https://doi.org/10.1007/s10064-019-01494-2>
- Qin T, Duan YW, Sun HR et al (2020) Mechanical characteristics and energy dissipation characteristics of sandstone under triaxial stress conditions. *J China Coal Soc* 45(S1):255–262. <https://doi.org/10.13225/j.cnki.jccs.2019.1393>
- Ranjith PG, Viète DR, Chen BJ et al (2012) Transformation plasticity and the effect of temperature on the mechanical behaviour of Hawkesbury sandstone at atmospheric pressure. *Eng Geol* 151:120–127. <https://doi.org/10.1016/j.enggeo.2012.09.007>
- Shao SH, Wu CL, Hao M, Song XL et al (2021) A novel coating technology for fast sealing of air leakage in underground coal mines. *Int J Min Sci Tech* 31(2):313–320. <https://doi.org/10.1016/j.ijmst.2020.08.004>
- Shen YJ, Hao JS, Hou X et al (2021) Crack propagation in high-temperature granite after cooling shock: experiment and numerical simulation. *Bull Eng Geol Environ* 80:5831–5844. <https://doi.org/10.1007/s10064-021-02259-6>
- Shen YJ, Hou X, Yuan JQ et al (2020) Thermal deterioration of high-temperature granite after cooling shock: multiple-identification and damage mechanism. *Bull Eng Geol Environ* 79:5385–5398. <https://doi.org/10.1007/s10064-020-01888-7>
- Shi BB, Su HT, Li JS et al (2017) Clean power generation from the intractable natural coalfield fires: Turn harm into benefit. *Science Report* 7(1):5302. <https://doi.org/10.1038/s41598-017-05622-4>
- Shi BB, Wang ZY, Liu P et al (2021) Pozzolanicity verification of combustion metamorphic rocks from coalfield fire zones in China. *J Loss Prev Process Ind* 69:104390. <https://doi.org/10.1016/j.jlpi.2021.104390>
- Shi XS, Jing HW, Yin Q et al (2020) Investigation on physical and mechanical properties of bedded sandstone after high-temperature exposure. *Bull Eng Geol Environ* 79(5):2591–2606. <https://doi.org/10.1007/s10064-020-01729-7>
- Sirdesai NN, Singh TN, Gamage RP (2017) Thermal alterations in the poro-mechanical characteristic of an Indian sandstone—a comparative study. *Eng Geol* 226:208–220. <https://doi.org/10.1016/j.enggeo.2017.06.010>
- Sun Q, Geng JS, Zhao F (2020) Experiment study of physical and mechanical properties of sandstone after variable thermal cycles. *Bull Eng Geol Environ* 79:3771–3784. <https://doi.org/10.1007/s10064-020-01779-x>
- Tao M, Meng XX, Zhang DH et al (2018) Using micro-computed tomography and scanning electron microscopy to assess the morphological evolution and fractal dimension of a salt-gypsum rock subjected to a coupled thermal-hydrological-chemical environment. *Mar Pet Geol* 98:316–334. <https://doi.org/10.1016/j.marpetgeo.2018.08.024>
- Wang EY, Jia HL, Song DZ et al (2014) Use of ultra-low-frequency electromagnetic emission to monitor stress and failure in coal mines. *Int J Rock Mech Min Sci* 70:16–25. <https://doi.org/10.1016/j.ijrmms.2014.02.004>
- Wang P, Xu JY, Fang XY et al (2017) Dynamic splitting tensile behaviors of red-sandstone subjected to repeated thermal shocks: deterioration and micro-mechanism. *Eng Geol* 223:1–10. <https://doi.org/10.1016/j.enggeo.2017.04.012>
- Wei SJ, Yang YS, Su CD et al (2019) Experimental study of the effect of high temperature on the mechanical properties of coarse sandstone. *Appl Sci-Basel* 9(12):2424. <https://doi.org/10.3390/app9122424>
- Xiao F, Jiang DY, Wu F et al (2021a) Effects of high temperature on the mechanical behaviors of sandstone under true-triaxial unloading conditions. *Bull Eng Geol Environ* 80(6):4587–4601. <https://doi.org/10.1007/s10064-021-02205-6>
- Xiao WJ, Zhang DM, Yang H et al (2021b) Laboratory investigation of the temperature influence on the mechanical properties and fracture crack distribution of rock under uniaxial compression test. *Bull Eng Geol Environ* 80(2):1585–1598. <https://doi.org/10.1007/s10064-020-01993-7>
- Xie HP, Li LY, Peng RD et al (2009) Energy analysis and criteria for structural failure of rocks. *J Rock Mech Geo Eng* 1(1):11–20. <https://doi.org/10.3724/SP.J.1235.2009.00011>
- Yavuz H, Demirdag S, Caran S (2010) Thermal effect on the physical properties of carbonate rocks. *Int J Rock Mech Min Sci* 47(1):94–103. <https://doi.org/10.1016/j.ijrmms.2009.09.014>
- Zhang H, Lu CP, Liu B et al (2020a) Numerical investigation on crack development and energy evolution of stressed coal-rock combination. *Int J Rock Mech Min Sci* 133:104417. <https://doi.org/10.1016/j.ijrmms.2020.104417>
- Zhang YL, Zhao GF, Qin L (2020b) Acoustic emission uncovers thermal damage evolution of rock. *Int J Rock Mech Min Sci* 132:104388. <https://doi.org/10.1016/j.ijrmms.2020.104388>
- Zhou FB, Shi BB, Cheng JW et al (2015) A new approach to control a serious mine fire with using liquid nitrogen as extinguishing media. *Fire Technol* 51:325–334. <https://doi.org/10.1007/s10694-013-0351-8>